JBC Papers in Press. Published on December 27, 2019 as Manuscript RA119.011699
The latest version is at http://www.jbc.org/cgi/doi/10.1074/jbc.RA119.011699

Activation of sphingosine 1-phosphate receptor 2 attenuates chemotherapy-induced neuropathy

Wei Wang[1,*], Ping Xiang[1,*], Wee Siong Chew[1], Federico Torta[2,3], Aishwarya Bandla[4], Violeta Lopez[5], Wei Lun Seow[1], Brenda Wan Shing Lam[1], Jing Kai Chang[1], Peiyan Wong[6], Kanokporn Chayaburakul[7], Wei-Yi Ong[8,9], Markus R. Wenk[2,3], Raghav Sundar[4, 10, 11, †], Deron R. Herr[1,12, †]

Department of Pharmacology[1], Singapore Lipidomics Incubator (SLING)[2], Department of Biochemistry[3], Alice Lee Centre for Nursing Studies[5], Neuroscience Phenotyping Core[6], Department of Anatomy[8], and Department of Medicine[10], Yong Loo Lin School of Medicine, National University of Singapore, Singapore;
The N.1 Institute for Health[4], and Neurobiology and Ageing Research Programme[9], National University of Singapore, Singapore
Anatomy Unit, Faculty of Science, Rangsit University, Thailand[7]
Department of Haematology-Oncology, National University Health System, Singapore[11]
Department of Biology, San Diego State University, San Diego, CA, U.S.A.[12]

Running title: *$S1P_2$ activation attenuates neuropathy*

* Wei Wang and Ping Xiang contributed equally.
† To whom correspondence should be addressed.
e-mail: phcdrh@nus.edu.sg and raghav_sundar@nuhs.edu.sg

Keywords: neuropathy, cisplatin, oxaliplatin, pharmacology, sphingosine 1-phosphate, G protein-coupled receptor, glial satellite cells, cancer, chemotherapy, antineoplastic drug

ABSTRACT

Platinum-based therapeutics are used to manage many forms of cancer, but frequently result in peripheral neuropathy. Currently, the only option available to attenuate chemotherapy-induced neuropathy is to limit or discontinue this treatment. Sphingosine 1-phosphate (S1P) is a lipid-based signaling molecule involved in neuroinflammatory processes by interacting with its five cognate receptors: $S1P_{1-5}$. In this study, using a combination of drug pharmacodynamics, analysis in human study participants, disease modeling in rodents, and cell-based assays, we examined whether S1P signaling may represent a potential target in the treatment of chemotherapy-induced neuropathy. To this end, we first investigated the effects of platinum-based drugs on plasma S1P levels in human cancer patients. Our analysis revealed that oxaliplatin treatment specifically increases one S1P species, d16:1 S1P, in these patients. Although d16:1 S1P is an $S1P_2$ agonist, it has lower potency than the most abundant S1P species (d18:1 S1P). Therefore, as d16:1 S1P concentration increases, it is likely to disproportionately activate proinflammatory $S1P_1$ signaling, shifting the balance away from $S1P_2$. We further show that a selective $S1P_2$ agonist, CYM-5478, reduces allodynia in a rat model of cisplatin-induced neuropathy and attenuates the associated inflammatory processes in the dorsal root ganglia, likely by activating stress response proteins, including ATF3 and HO-1. Cumulatively, the findings of our study suggest that the development of a specific $S1P_2$ agonist may represent a promising therapeutic approach for the management of chemotherapy-induced neuropathy.

Platinum-based chemotherapeutics, including cisplatin and oxaliplatin, are first-line antineoplastic drugs widely used for the treatment of many forms of cancer, including testicular, head and neck, lung, and cervical cancers (1-4). Unfortunately, cisplatin and oxaliplatin are also

associated with severe and potentially irreversible side effects, leading to dose-limiting modifications in treatment regimens (5,6). One of the most clinically significant, dose-limiting effect is neurotoxicity. Cisplatin-mediated neurotoxicity can present as peripheral sensory neuropathy, which is characterized by a variety of symptoms such as tingling paresthesia, burning pain, allodynia, and muscle weakness (7,8). Currently, there is no approved pharmacological method of attenuating cisplatin-mediated neuropathy, and toxic side effects are tolerated as an unfortunate consequence of life-saving chemotherapy. Studies have proposed various mechanisms to explain cisplatin-induced neuropathy, including the production of reactive oxygen species (ROS), inflammation, and activation of apoptotic pathways (9-11). Based on this mechanism, antioxidant therapy has been used for cisplatin-induced neuropathy in both preclinical models and clinical studies with some extent of protection (12-14). However, the use of broad-spectrum antioxidants has a number of shortcomings and is unlikely to be therapeutically useful as shown by the limited success of antioxidants in clinical trials (15,16). This may be due to the fact that antioxidant therapy is non-selective and broad suppression of endogenous oxidants may affect normal physiological signaling as well as interfere with the desired effects of cisplatin treatment (15). In addition, antioxidants can only scavenge existing ROS and are unable to undo any prior ROS damage to the cells (15). Therefore, a potential targeted therapy is needed for platinum-induced peripheral neuropathy.

Sphingosine 1-phosphate (S1P) is a potent signaling lipid that plays a role in many important cellular processes including cell proliferation, apoptosis, differentiation and cytoskeletal rearrangement (17,18). The effect of S1P is mediated by a family of five G protein-coupled receptors (GPCRs) termed S1P$_{1\text{-}5}$. These receptors are differentially expressed across various tissues and can activate a range of intracellular signaling cascades. Activation of S1P$_2$ in particular has been found to be associated with a variety of roles including modulating neuronal excitability, hepatocyte regeneration, muscle cell proliferation and differentiation, vascular permeability and anti-tumorigenic functions (19-24). The activation of RhoA and inhibition of Rac cascades are often coupled to S1P$_2$ activation in these roles. Notably, our group and others have established using S1P$_2$-knockout mice that S1P$_2$ has cytoprotective function toward the sensory neuroepithelial cells and afferent neurons of the cochlea (19,25,26), and that pharmacological activation of S1P$_2$ is associated with reduced ROS production and cytoprotection of neural cells (27). There is also evidence that S1P$_2$ is an important mediator of the development and differentiation of sensory cells of the cochlea (28,29).

Here, we report that the content of S1P is altered in the plasma of cancer patients treated with platinum-based chemotherapeutics. We further identify a mechanistic explanation for how the various S1P species may differentially contribute to these toxic side effects, reinforcing the importance of targeting S1P signaling. We then show that a specific S1P$_2$ agonist, CYM-5478, rescues genetic and phenotypic changes associated with cisplatin-mediated neuropathy, *in vivo*. Altogether, these results establish the S1P$_2$ receptor as a potential pharmacological target for the rescue of neurotoxic effects induced by platinum-based chemotherapeutics.

Results

Structural variants of S1P are selectively altered by platinum therapeutics

LC-MS/MS was used to quantify S1P (Figure 1A) in the plasma of cancer patients prior to and after an oxaliplatin treatment regimen. Although there was no change in total S1P concentration (Fig. 1B), when the 5 most abundant S1P species were considered individually, plasma levels of d16:1 S1P were significantly increased after oxaliplatin treatment (Fig. 1C). By contrast, the 4 remaining S1P species (d17:1 S1P, d18:0 S1P, d18:1 S1P, and d18:2 S1P) were unchanged (Fig. 1D-G).

To determine whether the specific alteration of d16:1 S1P may impact receptor-mediated S1P signaling, we performed the TGFα-shedding receptor activation assay (30). Interestingly, although we detected no difference in the potency of d16:1 S1P versus d18:1 S1P toward S1P$_1$ and S1P$_3$ (Fig. 1H&J), d16:1 S1P was significantly less potent toward S1P$_2$ (Fig. 1I). This suggests that an increase in d16:1

content would favor pro-inflammatory S1P$_1$ signaling (31) at the expense of S1P$_2$, suggesting that attenuation of S1P$_2$ signaling may contribute to peripheral neuropathy.

CYM-5478 attenuates cisplatin-mediated neuropathy in vivo

CYM-5478 (Fig. 2A) was identified in previous studies as a selective S1P$_2$ agonist (27,32). To determine if this tool compound was suitable for *in vivo* studies, we performed an *in vitro* metabolic stability assay using pooled male rat liver microsomes (MRLM) and female rat liver microsomes (FRLM) (Fig. 3B). Compared to the positive control compound which was rapidly metabolized, CYM-5478 was shown to be metabolically stable in the presence of FRLM ($t_{1/2}$ = 485.8±96.6 min), but rapidly metabolized by MRLM ($t_{1/2}$ = 8.90±0.1 min). This difference in metabolic stability is likely due to sex-specific differences in cytochrome P450 expression between male and female rat liver microsomes (33), and suggests that CYM-5478 may be suitable for *in vivo* specifically in female rats. To predict whether CYM-5478 was likely to be associated with significant toxicity over a 4-week period, the potential toxicity of CYM-5478 was studied in cell lines from various tissue origins, including liver, lung, colon, bone, cervix and prostate. Application of CYM-5478 had no significant effect on the viability of any cell line tested up to 100 μM, with the exception of HepG2 cells that demonstrated a minor loss of viability with an EC_{50} > 90 μM (Table 1). This suggests that CYM-5478 is unlikely to have significant acute toxicity *in vivo*.

Female SD rats were treated with cisplatin and CYM-5478 for three weeks (Fig. 3A). General toxicity for all rats was monitored by daily observation and measurement of body mass (Fig. 3B). In contrast to the control group which showed continuous weight gain over the study period, rats in the cisplatin group showed a reduction after each cisplatin dosing, which became significantly different from the control group from Day 15 (after the 3rd dose). Co-administration of CYM-5478 resulted in a delay in the loss of body mass, becoming statistically significant two days later than the cisplatin-only group. This suggests that CYM-5478, itself, does not result in general toxicity, and may attenuate the adverse effects of cisplatin.

Neuropathy was evaluated by behavioral manifestation of allodynia. Over the course of the study, the vehicle-treated control rats had no change in behavior, while all cisplatin-treated rats developed pronounced, progressive allodynia, consistent with neuropathy (Fig. 3C, Supplemental Fig. 2). The withdrawal time of rats in cisplatin group was significantly shorter after the first dose of cisplatin on Day 7, and became increasingly severe after each subsequent dose. This effect was significantly attenuated by co-administration of CYM-5478.

CYM-5478 attenuates cisplatin-induced myelin defects and glial activation

To determine the cellular processes underlying the behavioral phenotypes, dorsal roots and dorsal root ganglia (DRGs) were evaluated histologically (Fig. 4). Although there were no apparent morphological abnormalities of the DRGs (data not shown), axons in the dorsal root of cisplatin-treated rats were characterized by irregularities in their myelin sheaths. These irregularities were absent in cisplatin-treated rats that also received CYM-5478 (Fig. 4A-C). To better characterize these defects, dorsal root axons were examined by transmission electron microscopy (TEM) (Fig. 4D-I). Many axons from cisplatin-treated rats contained collapsed myelin structures resemble the widening of the Schmidt-Lanterman incisures seen in the early stages of axonal injury (34). Higher magnification revealed axons with widespread loss of myelin sheath integrity and disintegration of the axoplasm. These characteristics were largely absent from the axons of rats treated with both cisplatin and CYM-5478.

Since neuropathy is often characterized by activation of the glial satellite cells in the DRG (35) we evaluated glial fibrillary acidic protein (GFAP) reactivity by immunohistochemistry (Fig. 5). As expected, cisplatin treatment resulted in a significant increase in GFAP-positive cells. This increase was completely ameliorated by co-administration of CYM-5478, demonstrating that activation of S1P$_2$ is sufficient to prevent peripheral gliosis in this model.

To determine whether there was a direct effect of CYM-5478 on neuronal cells we used

differentiated PC12 cells to approximate neurons in vitro (36). Both cisplatin and CYM-5478 alone were sufficient to induce the expression of stress response genes *Atf3* and *Hmox1* (Figure 6A-B), presenting an apparent paradox. Interestingly, both of these genes are known to be induced by oxidative stress, and our previous work demonstrated that the protective effect of $S1P_2$ is likely to result from the attenuation of ROS (27). We reason that the cisplatin-mediated increase is an adaptive response to oxidative stress while CYM-5478 directly induces the repair response. To evaluate this, we quantified ROS with the CellROX assay. Indeed, as we have previously shown for C6 glioma cells (27) CYM-5478 results in a reduction, rather than an increase, of ROS in these neuronal-like cells (Figure 6C).

Discussion

Accumulation of ROS is known to play an important role in the pathophysiology of neuropathy. The involvement of S1P signaling in the regulation of ROS production has been demonstrated in the heart (37), isolated blood vessels (38), fibroblasts (39), and hematopoietic progenitor cells (40). Notably, our previous study confirmed that a deficiency of $S1P_2$ results in progressive and marked degeneration of the afferent neurons and neuroepithelial cells in the inner ear (25). We further demonstrated that $S1P_2$ knockout mice accumulate ROS in the spiral ganglia, likely leading to cytotoxic loss of afferent neurons, and that this accumulation could be attenuated *in vitro* by CYM-5478 (27). In the current study, i*n vivo* experiments showed that cisplatin-treated rats developed pronounced and progressive allodynia, consistent with neuropathy, which was significantly attenuated by co-administration of CYM-5478 (Fig. 3). This is the first *in vivo* study showing the neuroprotective effect by specific activation of $S1P_2$. It is important to take note, however, that impaired S1P signaling is not a prerequisite for CYM-5478 to exert its effects. Administration of CYM-5478 is a gain-of-function approach where the effects of CYM-5478 are mediated by *activation* of $S1P_2$ signaling and not by antagonizing a dysregulated signaling pathway. Thus, it is not necessary for S1P signaling to be dysregulated in various forms of neuropathy for CYM-5478 to be effective.

Our results on plasma of cancer patients prior to and after an oxaliplatin treatment regimen indicate that only plasma levels of d16:1 S1P were significantly increased after oxaliplatin treatment. This at first appears contrary to our observation that $S1P_2$ receptor activation has an anti-nociceptive effect. Nevertheless, our *in vitro* studies demonstrate that d16:1 has a higher potency for $S1P_1$ (Fig. 1H&I), thus favoring $S1P_1$ activation over the other S1P receptor isoforms. This is supported by the observation by another group, that d16:1 S1P had reduced potency and efficacy toward $S1P_2$ relative to the most abundant species, d18:1 S1P (41). It is possible that increased d16:1 SIP level in patients undergoing oxaliplatin treatment would favor the activation of $S1P_1$ receptors at the expense of $S1P_2$, resulting in a net pro-inflammatory or pro-oxidative stress effect. It should be noted, though, that d16:1 S1P comprises <10% of total plasma S1P content (42), so the potential physiological relevance of its homeostasis needs to be further clarified.

Previous work by the Salvemini lab has demonstrated that $S1P_1$ is involved in the development of chemotherapy-induced neuropathy (31,43), but unlike $S1P_2$, $S1P_1$ is a positive regulator of inflammation. Chemotherapy-induced neuropathy was shown to be associated with activation of the $S1P_1$ neuroinflammatory signaling pathway involving NF-κB and MAPK stimulation as well as the induction of inflammatory cytokines such as IL-1β (31). In addition, they showed that functional antagonism of $S1P_1$ with FTY720 attenuated chemotherapy-induced neuropathic pain due to paclitaxel, bortezomib, and oxaliplatin (31,43). While these previous studies identified $S1P_1$ as an important positive regulator of neuropathy, the current study demonstrates that $S1P_2$ antagonizes this effect. The antagonistic effect of these two S1P receptors contrasts our previous study that demonstrated a functionally redundant role of $S1P_2$ and $S1P_3$ in epithelial development (44), further exemplifying the complexity of the interactions among S1P receptors.

Satellite cells in the DRG may be activated by proinflammatory signaling, leading to neuropathic pain (35). The ability of CYM-5478 to block $S1P_2$ receptor signaling-induced inflammation / oxidative stress appears to be

distinct from the mechanism of action of cisplatin, which is believed to kill cancer cells by binding to DNA and interfering with its repair mechanism, eventually leading to cell death. This could point to the potential utility of this compound as a lead for development as an anti-neuropathic pain molecule.

Our results provide evidence for effects of $S1P_2$ on both glia (Figs. 4&5) and neurons (Fig. 6). While it is likely that $S1P_2$ is directly protective for multiple neural cell types, a recent study has identified a potential mechanism that may contribute to the efficacy of CYM-5478 in our model. Tran, et al utilized a primary cell co-culture model to demonstrate that $S1P_2$ attenuates neuronal excitotoxicity by inducing production of leukemia inhibitory factor in astrocytes (45), thus providing an indirect neuroprotective effect.

Interestingly, as further evidence for our conclusions, another independent group recently reported the anti-nociceptive effect of $S1P_2$ in a different model of neuropathy. Li, et al used a genetic gain-of-function/loss-of-function approach to demonstrate that $S1P_2$ activity attenuates ROS production and pain behavior in a rat model of mechanical allodynia (46).

In conclusion, our *in vivo* experiments have shown that promotion of $S1P_2$-mediated signaling with its selective agonist, CYM-5478, not only attenuated cisplatin-induced neuropathy, but also reduced renal toxicity. This is the first study that demonstrated the efficacy of CYM-5478 in attenuation of side effects induced by cisplatin-based chemotherapy. Compared with non-targeted antioxidants, $S1P_2$ receptor may be a more effective therapeutic target to reduce the side effects of platinum-based chemotherapeutics.

Experimental procedures

Recruitment of study patients

Patients were recruited from the National University Cancer Institute Cancer Centre with written informed consent prior to receiving neurotoxic chemotherapy. Blood as well as clinical information were collected from the patient before the start of chemotherapy, and at regular time points throughout chemotherapy, up to 12 months after the end of chemotherapy (Supplemental Fig. S1). Details have been previously reported (47). All human blood samples were collected in accordance to ethical guidelines and protocols. This study was approved by the National Healthcare Group Institutional Review Board (DSRB ref #2014/00646), Singapore and abides by the Declaration of Helsinki principles.

Lipid measurements

An internal standard (ISTD) for S1P analysis consisting of 20 ng/mL $^{13}C_2D_2$-S1P was first prepared in a mixture of buthanol:methanol (1:1). 10 µL of each plasma sample were then extracted in a randomized order as previously described (48). Briefly, 100 µL of the ISTD were added to the plasma samples and the samples were vortexed for 10 seconds before undergoing sonication for 30 min. Samples were then centrifuged at 16000 x g for 10 min at room temperature and 100 µL of the supernatant were transferred to a new tube for subsequent S1P derivatization as according to a previous protocol (42). 20 µL of TMS-diazomethane were added to the samples and the samples were then placed in a thermomixer at 1000 rpm for 20 min at room temperature. 1 µL of 10 % acetic acid was subsequently added to stop the derivatization reaction. The samples were then vortexed and centrifuged at 16000 x g for 10 min at room temperature and the supernatant containing the extracted lipids were then transferred into MS glass vials with Teflon insert caps. Samples were stored in -80 ºC until LC-MS lipidomic analysis. An Agilent 1290 UPLC system connected to an Agilent 6495 Triple Quadrupole mass spectrometer (Santa Clara, CA, USA) was used for the LC-MS analysis. The LC column used was an Acquity hydrophilic interaction chromatography (HILIC) column (100 x 2.1 mm, 1.7 µm particle size) (Waters Corporations, MA, USA) and the MS source parameters during the run were 200 ºC gas temperature and 400 ºC sheath gas temperature at a gas flow of 12 L/minute. Two mobile phases were used during the run which were Mobile Phase A (50 % acetonitrile in water with 25 mM ammonium formate) and Mobile Phase B (95 % acetonitrile in water with 25 mM ammonium formate). The mass spectrometer run was carried out in a positive ion MRM mode and five different S1P isoforms were quantified (S1P d16:1, S1P d17:1, S1P d18:0, S1P d18:1 and S1P d18:2). Lipidomic

data were then extracted and analyzed using Agilent MassHunter Qualitative and Agilent MassHunter Quantitative software (Santa Clara, CA, USA).

TGFα shedding assay

This assay was conducted essentially as described (30,49). Briefly, HEK293 cells were co-transfected with expression constructs for alkaline phosphatase-TGFα and the indicated receptor using Lipofectamine 3000 (cat # L3000015, Thermo Fisher). For $S1P_1$ and $S1P_2$ assays, cells were also co-transfected with a chimeric G protein (Gq/i1). Following a 24 h incubation they were collected by trypsinization, washed with 1x PBS, and seeded into 96-well plates in Hank's Balanced Saline Solution (HBSS). Stimulation with d16:1 and d18:1 S1P (Cayman chemicals, USA) was carried out for 1 h following which alkaline phosphatase activity was detected in both cells and supernatant. Activity of the receptor (% shedding) was described as the alkaline phosphatase activity of the supernatant/total alkaline phosphatase activity (cells + supernatant). Values were normalized to basal activity of unstimulated cells to control for variations in transgene expression. Data processing and statistical analyses were performed with GraphPad Prism 7.

In vitro metabolic stability assay

Liver microsomal incubations were conducted in triplicate. Incubation mixtures consisted of microsomes (0.3 mg protein/mL) and CYM-5478 (1 µM) in 0.1 M phosphate buffer (pH 7.4). The mixture was first shaken for 5 min for pre-incubation in a shaking water bath at 37ºC. Reaction was initiated by adding 50 NADPH to a final concentration of 1 mM. Aliquots (50 µL) of the incubation sample mixture were collected at 0, 5, 10, 15, 30, and 45 min. After collection, the reaction was terminated with 100 µL of chilled acetonitrile containing the internal standard (0.9 µM USA-109). The mixture was then centrifuged at 10,000 X g to remove the protein and the supernatant was subsequently applied to LC-MS/MS analysis. Positive control (PC) samples were prepared as described above, except the test compound was replaced with the known P450 substrate (Midazolam, 3 µM). The samples were assayed for the degradation of midazolam to evaluate the adequacy of the experimental conditions for drug metabolism study. Quantitation of compounds was performed with an LC-MS/MS system composed of Agilent 1290 Infinity HPLC system (Agilent Technology, Waldbronn, Germany) coupled to a Q TrapTM 5500 hybrid triple quadrupole linear ion trap mass spectrometer (Applied Biosystems/MDS Sciex, Concord, Ontario, Canada). Chromatographic separation was performed on a Zorbax Eclipse Plus C18 column (2.1X 100 mm, i.d., 3.5 µm, Agilent Technologies, Palo Alto, CA, USA) with a Security Guard Cartridge (3.0 X 4 mm, Agilent Technologies, Palo Alto, CA, USA). The mobile phase consisted of acetonitrile containing 0.1% formic acid - water containing 0.1% formic acid and the flow rate was set at 0.4 mL/min and the column temperature was ambient. The mass spectrometer was operated using ESI source in the positive ion detection mode. In the determination of the *in vitro* half-life ($T_{1/2}$), the peak areas of drug were converted to parent remaining percentages, using the t = 0 peak area values as 100%. Data points were the average of three measurements with standard deviations as the error bars. The *in vitro* $T_{1/2}$ was calculated from the slope of the linear regression (k) of the natural logarithm of the parent remaining percentage versus incubation time according to the following formula as described previously (50).

In vitro cytotoxicity

Cell lines used: DU145 human prostate cancer (ATCC #HTB-81), A549 human lung cancer (ATCC #CRM-CCL-185), HCT116 human colon cancer (ATCC #CCL-247), U2OS human bone osteosarcoma (ATCC #HTB-96), HeLa human cervix cancer (ATCC #CCL-2), HepG2 human liver cancer (ATCC #HB-8065). All cells lines were grown in Dulbecco's modified Eagle's medium (DMEM) supplemented with 10% fetal bovine serum (Hyclone, USA) and 2 mM Glutamine (Thermo Fisher, USA). Cells were seeded on culture dishes at a density of 25×10^3 cells/cm^2 and incubated at 37 °C in 5% CO_2. Cell growth inhibitory effect of was measured using a colorimetric MTT assay reagent (Sigma Aldrich, USA). Cancer cells were plated in 96-well plates at a density of 2,000 –

3,000 cells/well (N = 3-5). The cells were incubated for 24 h without treatment and for 72 h with drug, after which the drug solution was removed, 100µl of MTT dye (3-[4, 5-dimethylthiazol-2-yl]- 2, 5-diphenyl tetrazolium bromide, 0.5 mg/ml in DMEM), was added to each well, and the plates were incubated for 1-3 h at 37ºC. Then, the media was aspirated, and 100 µl DMSO was added to each well to solubilize the formant crystals. The absorbance was measured at a wavelength of 570 nm.

Animals

Female Sprague-Dawley rats weighing about 200 g (InVivos, Singapore) were used in the study. Animals were housed in groups of 2 per cage and maintained in a 12 h light/dark cycle (lights on and off at 7:00 and 19:00, respectively) in a temperature (22–24 °C) and humidity (45–55%) controlled facility. Standard chow and water were provided *ad libitum*. Each treatment group contained 4 rats and was repeated in a second, identical batch one month later (N = 8 per group). The experimental procedures were approved by the Institutional Animal Care and Use Committee (IACUC) at the National University of Singapore.

Drug treatment

Cisplatin (C2210000, Sigma Aldrich, USA) was freshly prepared before each use by dissolving in sterile saline. 3 mg/kg was administered intraperitoneally (i.p.) at 2 mL/kg to the rats once a week (days 0, 7, and 14). The dose of cisplatin which induced peripheral neuropathy was referenced from previous study in rats (51). CYM-5478 (MolPort-004-121-217, MolPort, Latvia) was prepared weekly by dissolving in 100% dimethyl sulfoxide (DMSO) at 10 mg/mL. Before each use, the DMSO stock was diluted in saline containing 0.1% TWEEN-20. 0.1 mg/mL was administered i.p. at 1mg/kg every day. The treatment started on day -1 (Figure 2). Drug administrations were controlled so that all rats received identical vehicle treatments.

von Frey test

Mechanical allodynia was measured by the von Frey test on Days -1, 6, 13, and 20 (Fig. 3) with a protocol modified from a previous study (52). Each rat was placed on a wire mesh floor covered by a transparent Plexiglas cage. On the week before the first drug administration, rats were placed in the test environment each day for 15 min. For testing, rats were allowed to acclimate for 10 min before measuring hind paw mechanical thresholds. A single, un-bending electronic filament that administered stimuli between 1-40 g in ascending increments of 5 g, was applied to the middle of the plantar surface of the left hind paw and held for 1 second or until a pain-evoked paw withdrawal ("withdrawal time") was observed. 1 second was set as the cut-off for each measurement. The duration until paw withdrawal was measured 5 times at each specific force. The experiments were repeated with the right hind paw.

Transmission electron microscopy

Freshly isolated DRGs with associated dorsal roots were fixed in 2% paraformaldehyde and 3% glutaraldehyde in 0.1 M PBS overnight at 4 ºC, post-fixed with 1% OsO_4 for 1.5 h, dehydrated in an ascending series of ethanol and acetone, and embedded in Araldite. Semi-thin sections were obtained before collecting ultrathin sections on Formvar coated copper grids. The sections were stained with uranyl acetate, and examined using a Joel 1010 transmission electron microscope (JEOL, Japan).

Immunohistochemistry

The DRGs and associated dorsal roots were excised, fixed in 4% ice-cold paraformaldehyde, dehydrated though an ethanol series, embedded in paraffin, cut at 5 µm thickness, and collected on Superfrost Plus slides (Thermo Fisher). Antigen retrieval was performed by incubating slides in 0.1 M Tris, pH 9.0 in a boiling water bath for 20 min. Slides were then blocked with 2.5% BSA/0.1% Triton-X 100 for 30 min, incubated with α-GFAP (Santa Cruz Biotechnology #sc-33673) diluted 1:150 in blocking buffer at 4 ºC overnight, washed 3 times in 1X PBS, incubated with Goat anti-Mouse IgG Alexafluor 488-conjugated secondary antibody (Thermo Fisher #32723) diluted 1:250 in blocking buffer for 2 h, washed 3 times in 1X PBS, and mounted with Vectashield (Vector Laboratories # H-1000). Images were captured with an epifluorescence microscope at 20X

magnification and scored for GFAP immunoreactivity by a blinded researcher.

Cell culture

PC12 cells (ATCC # CRL-1721) were maintained as subconfluent monolayers in Dulbecco's Modified Eagle Medium (DMEM) high glucose (Thermo Fisher #11965167) containing 10% fetal bovine serum (Thermo Fisher #16000044). Cells were differentiated in DMEM + 1% horse serum + 50 ng/ml nerve growth factor for 7 days essentially as described (36).

Quantitative real-time-PCR (qRT-PCR)

qRT-PCR was performed essentially as described (53). Briefly, total RNA was isolated using TRIzol reagent (Thermo Fisher #15596018), and used for synthesis of complementary DNA using the Maxima First Strand cDNA Synthesis Kit (Thermo Fisher #K1641). Real-time-PCR to amplify targets was performed using Maxima SYBR Green/ROX qPCR Master Mix (Thermo Fisher #K0223) with the QuantStudio 6 Flex Real-Time PCR System (Thermo Fisher Scientific, USA) using the following specific primer sets: *Gapdh* (forward 5'-TGATGGGTGTGAACCACGAG-3', reverse 5'-TCATGAGCCCTTCCACGATG-3'), *Hmox1* (forward 5'-ATCCCTTACACACCAGCCAC-3', reverse 5'-TCCAGAGTGTTCATGCGAGC-3'), *Atf3* (forward 5'-TGTCAGTCACCAAGTCTGAGG-3', reverse 5'-CTCTCCAGTTTCTCTGACTCCTTC-3'). Data were analyzed using the $2^{-\Delta\Delta Ct}$ method.

Statistical analyses

All tests for significance were performed by ordinary one-way ANOVA followed by Tukey's multiple comparison test on Graphpad Prism software version 7 or 8. Differences were considered significant when $P < 0.05$. Error bars indicate standard deviations unless stated otherwise. Sample sizes for each experiment are described in figure legends and in Supplemental Table S1. All P-values and F-statistics are provided in Supplemental Table S1.

Acknowledgments/grant support: The authors would like to thank A/Prof Go Mei Lin and the Drug Development Unit at NUS for assistance in compound characterization. This work was supported by the Ministry of Education, Singapore (T1-2013Sep-09, DRH), and the National University Health System (NUHSRO/2014/085/AF-Partner/01, DRH and NUHSRO/2017/064/Bridging/02, DRH). The behavioral experiments were carried out at the Neuroscience Phenotyping Core Facility, which is supported by the NMRC NUHS Centre Grant (NMRC/CG/M009/2017_NUH/NUHS).

Conflict of interest: The authors declare that they have no conflicts of interest with the contents of this article.

References

1. Einhorn, L. H. (2002) Curing metastatic testicular cancer. *Proc Natl Acad Sci U S A* **99**, 4592-4595

2. Colevas, A. D., Lira, R. R., Colevas, E. A., Lavori, P. W., Chan, C., Shultz, D. B., and Chang, K. W. (2015) Hearing evaluation of patients with head and neck cancer: Comparison of Common Terminology Criteria for Adverse Events, Brock and Chang adverse event criteria in patients receiving cisplatin. *Head Neck* **37**, 1102-1107

3. Masters, G. A., Temin, S., Azzoli, C. G., Giaccone, G., Baker, S., Jr., Brahmer, J. R., Ellis, P. M., Gajra, A., Rackear, N., Schiller, J. H., Smith, T. J., Strawn, J. R., Trent, D., Johnson, D. H., and American Society of Clinical Oncology Clinical, P. (2015) Systemic Therapy for Stage IV Non-Small-Cell Lung Cancer: American Society of Clinical Oncology Clinical Practice Guideline Update. *J Clin Oncol* **33**, 3488-3515

4. Li, H., Wu, X., and Cheng, X. (2016) Advances in diagnosis and treatment of metastatic cervical cancer. *J Gynecol Oncol* **27**, e43

5. Hartmann, J. T., and Lipp, H. P. (2003) Toxicity of platinum compounds. *Expert Opin Pharmacother* **4**, 889-901

6. Sastry, J., and Kellie, S. J. (2005) Severe neurotoxicity, ototoxicity and nephrotoxicity following high-dose cisplatin and amifostine. *Pediatr Hematol Oncol* **22**, 441-445

7. Seretny, M., Currie, G. L., Sena, E. S., Ramnarine, S., Grant, R., MacLeod, M. R., Colvin, L. A., and Fallon, M. (2014) Incidence, prevalence, and predictors of chemotherapy-induced peripheral neuropathy: A systematic review and meta-analysis. *Pain* **155**, 2461-2470

8. Akman, T., Akman, L., Erbas, O., Terek, M. C., Taskiran, D., and Ozsaran, A. (2015) The preventive effect of oxytocin to Cisplatin-induced neurotoxicity: an experimental rat model. *Biomed Res Int* **2015**, 167235

9. Karasawa, T., and Steyger, P. S. (2015) An integrated view of cisplatin-induced nephrotoxicity and ototoxicity. *Toxicol Lett* **237**, 219-227

10. Dasari, S., and Tchounwou, P. B. (2014) Cisplatin in cancer therapy: molecular mechanisms of action. *Eur J Pharmacol* **740**, 364-378

11. Kelley, M. R., Jiang, Y., Guo, C., Reed, A., Meng, H., and Vasko, M. R. (2014) Role of the DNA base excision repair protein, APE1 in cisplatin, oxaliplatin, or carboplatin induced sensory neuropathy. *PLoS One* **9**, e106485

12. Gutierrez-Gutierrez, G., Sereno, M., Miralles, A., Casado-Saenz, E., and Gutierrez-Rivas, E. (2010) Chemotherapy-induced peripheral neuropathy: clinical features, diagnosis, prevention and treatment strategies. *Clin Transl Oncol* **12**, 81-91

13. Pace, A., Giannarelli, D., Galie, E., Savarese, A., Carpano, S., Della Giulia, M., Pozzi, A., Silvani, A., Gaviani, P., Scaioli, V., Jandolo, B., Bove, L., and Cognetti, F. (2010) Vitamin E neuroprotection for cisplatin neuropathy: a randomized, placebo-controlled trial. *Neurology* **74**, 762-766

14. Joseph, E. K., and Levine, J. D. (2009) Comparison of oxaliplatin- and cisplatin-induced painful peripheral neuropathy in the rat. *J Pain* **10**, 534-541

15. Giordano, S., Darley-Usmar, V., and Zhang, J. (2014) Autophagy as an essential cellular antioxidant pathway in neurodegenerative disease. *Redox Biol* **2**, 82-90

16. Areti, A., Yerra, V. G., Naidu, V., and Kumar, A. (2014) Oxidative stress and nerve damage: role in chemotherapy induced peripheral neuropathy. *Redox Biol* **2**, 289-295

17. Hannun, Y. A., and Obeid, L. M. (2008) Principles of bioactive lipid signalling: lessons from sphingolipids. *Nat Rev Mol Cell Biol* **9**, 139-150

18. Gardell, S. E., Dubin, A. E., and Chun, J. (2006) Emerging medicinal roles for lysophospholipid signaling. *Trends Mol Med* **12**, 65-75

19. MacLennan, A. J., Carney, P. R., Zhu, W. J., Chaves, A. H., Garcia, J., Grimes, J. R., Anderson, K. J., Roper, S. N., and Lee, N. (2001) An essential role for the H218/AGR16/Edg-5/LP(B2) sphingosine 1-phosphate receptor in neuronal excitability. *Eur J Neurosci* **14**, 203-209

20. Ikeda, H., Watanabe, N., Ishii, I., Shimosawa, T., Kume, Y., Tomiya, T., Inoue, Y., Nishikawa, T., Ohtomo, N., Tanoue, Y., Iitsuka, S., Fujita, R., Omata, M., Chun, J., and Yatomi, Y. (2009) Sphingosine 1-phosphate regulates regeneration and fibrosis after liver injury via sphingosine 1-phosphate receptor 2. *J Lipid Res* **50**, 556-564

21. Grabski, A. D., Shimizu, T., Deou, J., Mahoney, W. M., Jr., Reidy, M. A., and Daum, G. (2009) Sphingosine-1-phosphate receptor-2 regulates expression of smooth muscle alpha-actin after arterial injury. *Arterioscler Thromb Vasc Biol* **29**, 1644-1650

22. Loh, K. C., Leong, W. I., Carlson, M. E., Oskouian, B., Kumar, A., Fyrst, H., Zhang, M., Proia, R. L., Hoffman, E. P., and Saba, J. D. (2012) Sphingosine-1-phosphate enhances satellite cell activation in dystrophic muscles through a S1PR2/STAT3 signaling pathway. *PLoS One* **7**, e37218

23. Sanchez, T., Skoura, A., Wu, M. T., Casserly, B., Harrington, E. O., and Hla, T. (2007) Induction of vascular permeability by the sphingosine-1-phosphate receptor-2 (S1P2R) and its downstream effectors ROCK and PTEN. *Arterioscler Thromb Vasc Biol* **27**, 1312-1318

24. Adada, M., Canals, D., Hannun, Y. A., and Obeid, L. M. (2013) Sphingosine-1-phosphate receptor 2. *FEBS J* **280**, 6354-6366

25. Herr, D. R., Grillet, N., Schwander, M., Rivera, R., Muller, U., and Chun, J. (2007) Sphingosine 1-phosphate (S1P) signaling is required for maintenance of hair cells mainly via activation of S1P2. *J Neurosci* **27**, 1474-1478

26. Kono, M., Belyantseva, I. A., Skoura, A., Frolenkov, G. I., Starost, M. F., Dreier, J. L., Lidington, D., Bolz, S. S., Friedman, T. B., Hla, T., and Proia, R. L. (2007) Deafness and stria vascularis defects in S1P2 receptor-null mice. *J Biol Chem* **282**, 10690-10696

27. Herr, D. R., Reolo, M. J., Peh, Y. X., Wang, W., Lee, C. W., Rivera, R., Paterson, I. C., and Chun, J. (2016) Sphingosine 1-phosphate receptor 2 (S1P2) attenuates reactive oxygen species formation and inhibits cell death: implications for otoprotective therapy. *Sci Rep* **6**, 24541

28. Cencetti, F., Bernacchioni, C., Bruno, M., Squecco, R., Idrizaj, E., Berbeglia, M., Bruni, P., and Donati, C. (2019) Sphingosine 1-phosphate-mediated activation of ezrin-radixin-moesin proteins contributes to cytoskeletal remodeling and changes of membrane properties in epithelial otic vesicle progenitors. *Biochim Biophys Acta Mol Cell Res* **1866**, 554-565

29. Bruno, G., Cencetti, F., Bernacchioni, C., Donati, C., Blankenbach, K. V., Thomas, D., Meyer Zu Heringdorf, D., and Bruni, P. (2018) Bradykinin mediates myogenic differentiation in murine myoblasts through the involvement of SK1/Spns2/S1P2 axis. *Cell Signal* **45**, 110-121

30. Inoue, A., Ishiguro, J., Kitamura, H., Arima, N., Okutani, M., Shuto, A., Higashiyama, S., Ohwada, T., Arai, H., Makide, K., and Aoki, J. (2012) TGFalpha shedding assay: an accurate and versatile method for detecting GPCR activation. *Nat Methods* **9**, 1021-1029

31. Janes, K., Little, J. W., Li, C., Bryant, L., Chen, C., Chen, Z., Kamocki, K., Doyle, T., Snider, A., Esposito, E., Cuzzocrea, S., Bieberich, E., Obeid, L., Petrache, I., Nicol, G., Neumann, W. L., and Salvemini, D. (2014) The development and maintenance of paclitaxel-induced neuropathic pain require activation of the sphingosine 1-phosphate receptor subtype 1. *J Biol Chem* **289**, 21082-21097

32. Satsu, H., Schaeffer, M. T., Guerrero, M., Saldana, A., Eberhart, C., Hodder, P., Cayanan, C., Schurer, S., Bhhatarai, B., Roberts, E., Rosen, H., and Brown, S. J. (2013) A sphingosine 1-phosphate receptor 2 selective allosteric agonist. *Bioorg Med Chem* **21**, 5373-5382

33. Kato, R., and Yamazoe, Y. (1992) Sex-specific cytochrome P450 as a cause of sex- and species-related differences in drug toxicity. *Toxicol Lett* **64-65 Spec No**, 661-667

34. Wong, K. M., Babetto, E., and Beirowski, B. (2017) Axon degeneration: make the Schwann cell great again. *Neural Regen Res* **12**, 518-524

35. Ohara, P. T., Vit, J. P., Bhargava, A., Romero, M., Sundberg, C., Charles, A. C., and Jasmin, L. (2009) Gliopathic pain: when satellite glial cells go bad. *Neuroscientist* **15**, 450-463

36. Zhou, T., Xu, B., Que, H., Lin, Q., Lv, S., and Liu, S. (2006) Neurons derived from PC12 cells have the potential to develop synapses with primary neurons from rat cortex. *Acta Neurobiol Exp (Wars)* **66**, 105-112

37. Takuwa, N., Ohkura, S., Takashima, S., Ohtani, K., Okamoto, Y., Tanaka, T., Hirano, K., Usui, S., Wang, F., Du, W., Yoshioka, K., Banno, Y., Sasaki, M., Ichi, I., Okamura, M., Sugimoto, N., Mizugishi, K., Nakanuma, Y., Ishii, I., Takamura, M., Kaneko, S., Kojo, S., Satouchi, K., Mitumori, K., Chun, J., and Takuwa, Y. (2010) S1P3-mediated cardiac fibrosis in sphingosine kinase 1 transgenic mice involves reactive oxygen species. *Cardiovasc Res* **85**, 484-493

38. Keller, M., Lidington, D., Vogel, L., Peter, B. F., Sohn, H. Y., Pagano, P. J., Pitson, S., Spiegel, S., Pohl, U., and Bolz, S. S. (2006) Sphingosine kinase functionally links elevated transmural pressure and increased reactive oxygen species formation in resistance arteries. *FASEB J* **20**, 702-704

39. Catarzi, S., Giannoni, E., Favilli, F., Meacci, E., Iantomasi, T., and Vincenzini, M. T. (2007) Sphingosine 1-phosphate stimulation of NADPH oxidase activity: relationship with platelet-derived growth factor receptor and c-Src kinase. *Biochim Biophys Acta* **1770**, 872-883

40. Golan, K., Vagima, Y., Ludin, A., Itkin, T., Cohen-Gur, S., Kalinkovich, A., Kollet, O., Kim, C., Schajnovitz, A., Ovadya, Y., Lapid, K., Shivtiel, S., Morris, A. J., Ratajczak, M. Z., and Lapidot, T. (2012) S1P promotes murine progenitor cell egress and mobilization via S1P1-mediated ROS signaling and SDF-1 release. *Blood* **119**, 2478-2488

41. Troupiotis-Tsailaki, A., Zachmann, J., Gonzalez-Gil, I., Gonzalez, A., Ortega-Gutierrez, S., Lopez-Rodriguez, M. L., Pardo, L., and Govaerts, C. (2017) Ligand chain length drives activation of lipid G protein-coupled receptors. *Sci Rep* **7**, 2020

42. Narayanaswamy, P., Shinde, S., Sulc, R., Kraut, R., Staples, G., Thiam, C. H., Grimm, R., Sellergren, B., Torta, F., and Wenk, M. R. (2014) Lipidomic "deep profiling": an enhanced workflow to reveal new molecular species of signaling lipids. *Anal Chem* **86**, 3043-3047

43. Stockstill, K., Doyle, T. M., Yan, X., Chen, Z., Janes, K., Little, J. W., Braden, K., Lauro, F., Giancotti, L. A., Harada, C. M., Yadav, R., Xiao, W. H., Lionberger, J. M., Neumann, W. L., Bennett, G. J., Weng, H. R., Spiegel, S., and Salvemini, D. (2018) Dysregulation of sphingolipid metabolism contributes to bortezomib-induced neuropathic pain. *J Exp Med* **215**, 1301-1313

44. Herr, D. R., Lee, C. W., Wang, W., Ware, A., Rivera, R., and Chun, J. (2013) Sphingosine 1-phosphate receptors are essential mediators of eyelid closure during embryonic development. *J Biol Chem* **288**, 29882-29889

45. Tran, C., Heng, B., Teo, J. D., Humphrey, S. J., Qi, Y., Couttas, T. A., Stefen, H., Brettle, M., Fath, T., Guillemin, G. J., and Don, A. S. (2019) Sphingosine 1-phosphate but not Fingolimod protects neurons against excitotoxic cell death by inducing neurotrophic gene expression in astrocytes. *J Neurochem*

46. Li, Y., Li, H., and Han, J. (2019) Sphingosine-1-phosphate receptor 2 modulates pain sensitivity by suppressing the ROS-RUNX3 pathway in a rat model of neuropathy. *J Cell Physiol*

47. Molassiotis, A., Cheng, H. L., Lopez, V., Au, J. S. K., Chan, A., Bandla, A., Leung, K. T., Li, Y. C., Wong, K. H., Suen, L. K. P., Chan, C. W., Yorke, J., Farrell, C., and Sundar, R. (2019) Are we mis-estimating chemotherapy-induced peripheral neuropathy? Analysis of assessment methodologies from a prospective, multinational, longitudinal cohort study of patients receiving neurotoxic chemotherapy. *BMC Cancer* **19**, 132

48. Burla, B., Muralidharan, S., Wenk, M. R., and Torta, F. (2018) Sphingolipid Analysis in Clinical Research. *Methods Mol Biol* **1730**, 135-162

49. Thirunavukkarasan, M., Wang, C., Rao, A., Hind, T., Teo, Y. R., Siddiquee, A. A., Goghari, M. A. I., Kumar, A. P., and Herr, D. R. (2017) Short-chain fatty acid receptors inhibit invasive phenotypes in breast cancer cells. *PLoS One* **12**, e0186334

50. Lu, C., Li, P., Gallegos, R., Uttamsingh, V., Xia, C. Q., Miwa, G. T., Balani, S. K., and Gan, L. S. (2006) Comparison of intrinsic clearance in liver microsomes and hepatocytes from rats and humans: evaluation of free fraction and uptake in hepatocytes. *Drug Metab Dispos* **34**, 1600-1605

51. Authier, N., Gillet, J. P., Fialip, J., Eschalier, A., and Coudore, F. (2003) An animal model of nociceptive peripheral neuropathy following repeated cisplatin injections. *Exp Neurol* **182**, 12-20

52. Chaplan, S. R., Bach, F. W., Pogrel, J. W., Chung, J. M., and Yaksh, T. L. (1994) Quantitative assessment of tactile allodynia in the rat paw. *J Neurosci Methods* **53**, 55-63

53. Wang, W., Hind, T., Lam, B. W. S., and Herr, D. R. (2019) Sphingosine 1-phosphate signaling induces SNAI2 expression to promote cell invasion in breast cancer cells. *FASEB J* **33**, 7180-7191

Table 1: *In vitro* toxicity of CYM-5478

Cell Line	**Tissue**	**EC_{50}**
HepG2	Liver	92.92µM
A549	Lung	>50µM *
HCT116	Colon	>100µM
U2OS	Bone	>100µM
HeLa	Cervix	>100µM
DU145	Prostate	>100µM
*The highest concentration used for A549 was 50µM		

Figures

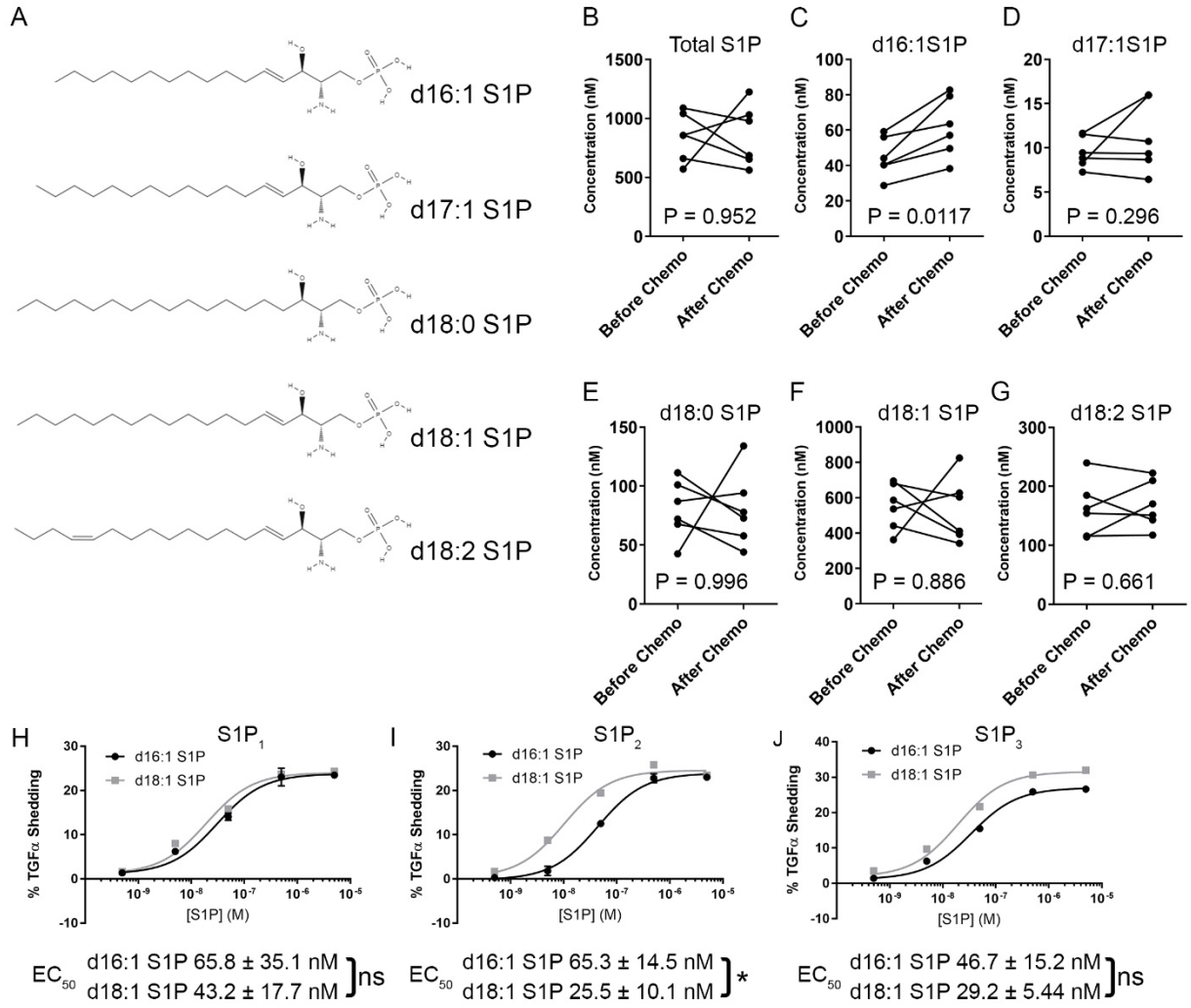

Figure 1: Oxaliplatin therapy alters S1P signaling in cancer patients. (A) This study evaluated the 5 most abundant variants of S1P in human plasma. Total S1P (B) and each individual species (C-G) were quantified by mass spectroscopy before and after an oxaliplatin regimen. (H-J) The activity of d16:1 S1P was compared to that of the most abundant form, d18:1 S1P, against $S1P_1$ (H), $S1P_2$ (I), and $S1P_3$ (J). N = 6 patients (B-G), N = 3 (H-J), EC_{50} values represent the mean of 3 independent experiments, *P < 0.05, ns = not significant. Error bars represent standard deviations of triplicate samples within an independent experiment.

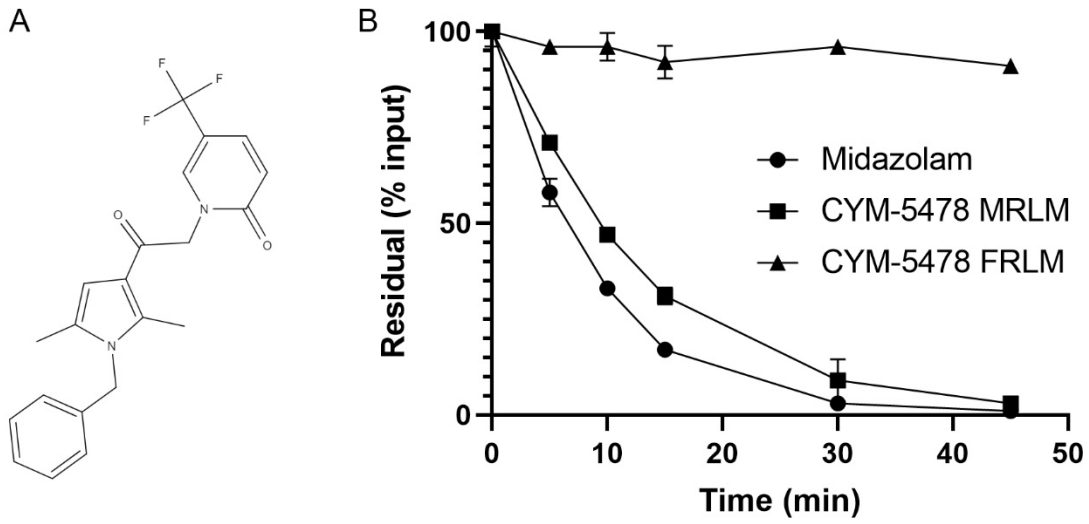

Figure 2: CYM-5478 is suitable for use in female rats *in vivo*. (A) Structure of CYM-5478. (B) The metabolic stability of CYM-5478 was approximated with microsomal stability assay. CYM-5478 was incubated with microsomal fractions prepared from the livers of male (MRLM) or female (FRLM) rats and evaluated for loss of parent compound by mass spectrometry. Midazolam was used as a positive control substrate due to its known rapid metabolism in this assay. N = 3. Error bars represent standard deviations.

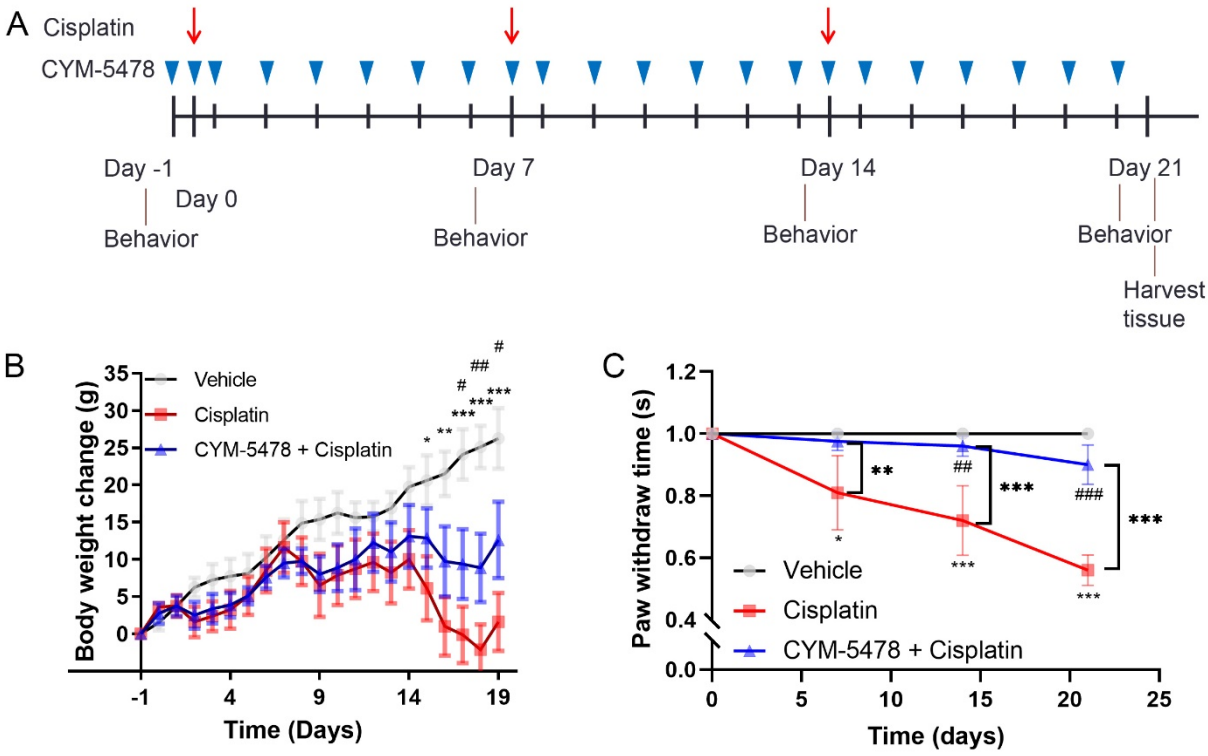

Figure 3: CYM-5478 attenuates cisplatin-mediated toxicity. (A) Graphic depiction of the experimental design. (B) Rats in each group were weighed daily as a general assessment of overall health. Total body mass gain is depicted as the change from the start of the study. (C) Behavioral assessment of neuropathy was determined by the plantar Von Frey filament assay. Rats were probed on the left rear foot pad with an Von Frey filament calibrated to deliver a force of 40g for 1 second. Time to withdrawal was captured by the electronic filament and recorded. Trials that did not elicit a response were given a value of 1. N = 8 rats per group. * = significance relative to vehicle control. # = significance relative to cisplatin-treated group. *P < 0.05, **P < 0.01, ***P < 0.001. Error bars represent standard deviations.

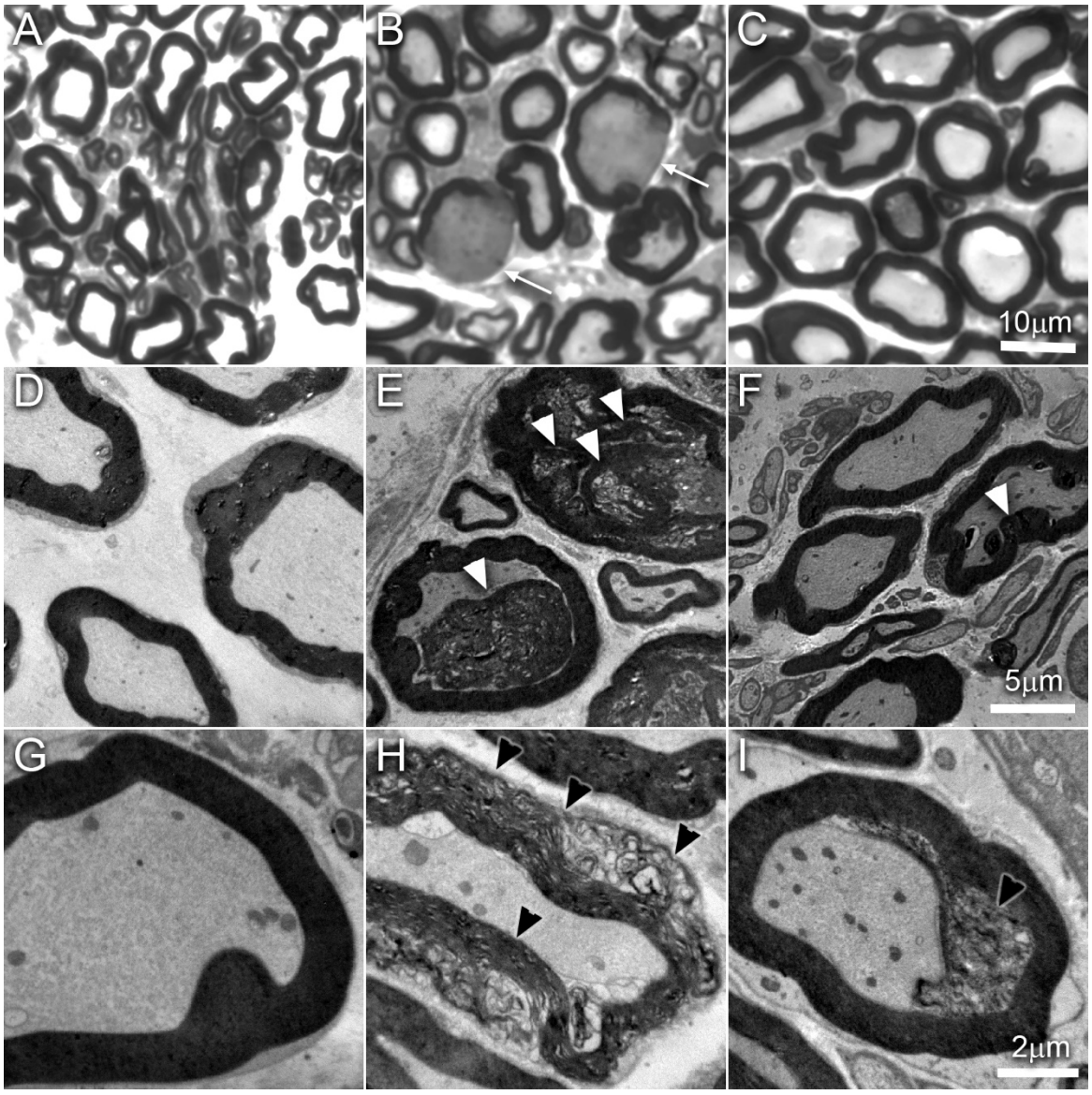

Figure 4: Cisplatin-induced myelination defects in dorsal root axons. (A-C) Micrographs of toluidine blue-stained semi-thin sections of the dorsal root taken from rats treated with vehicle (A), cisplatin (B), and CYM-5478 + cisplatin (C) at 40X magnification. Arrows indicate visible lesions in the myelin sheaths. (D-E) TEM images of the dorsal root taken from rats treated with vehicle (D), cisplatin (E), and CYM-5478 + cisplatin (F) at 3,000X magnification. White arrowheads indicate areas of collapsed myelin. (G-I) TEM images of the dorsal root taken from rats treated with vehicle (G), cisplatin (H), and CYM-5478 + cisplatin (I) at 6,000X magnification. Black arrowheads indicate areas of myelin sheath disintegration.

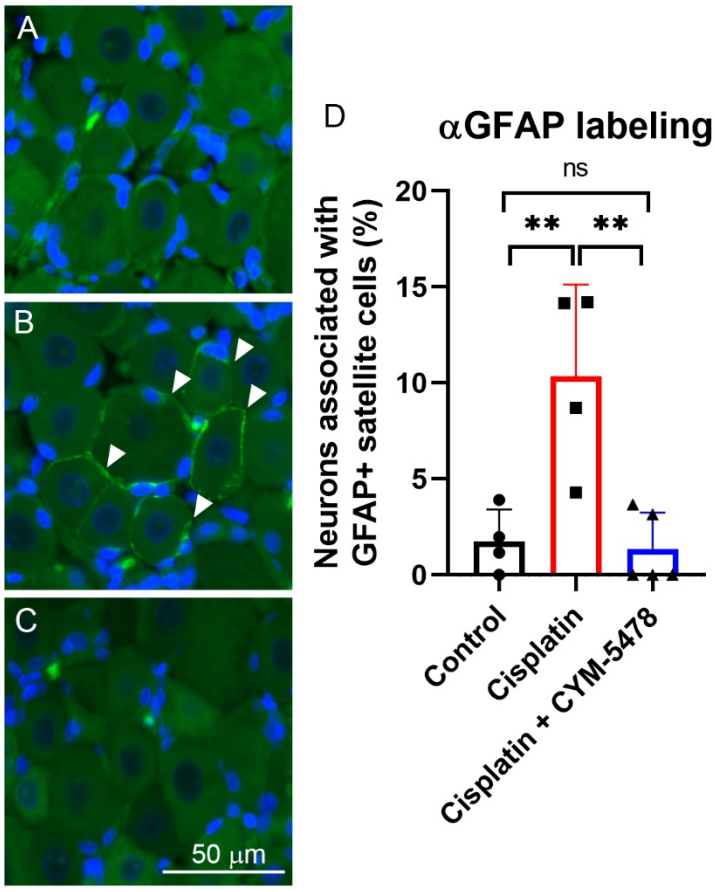

Figure 5: Evaluation of activated glial satellite cells in the DRG. (A-C) Micrographs of α-GFAP-labeled DRG sections taken from rats treated with vehicle (A), cisplatin (B), and CYM-5478 + cisplatin (C) at 40X magnification. (D) GFAP immunoreactivity quantified by counting the number of neurons ensheathed by GFAP+ glial satellite cells as percent of total neurons. N = 4-5 animals per group, >100 cells per individual. **P < 0.01. Error bars represent standard deviations.

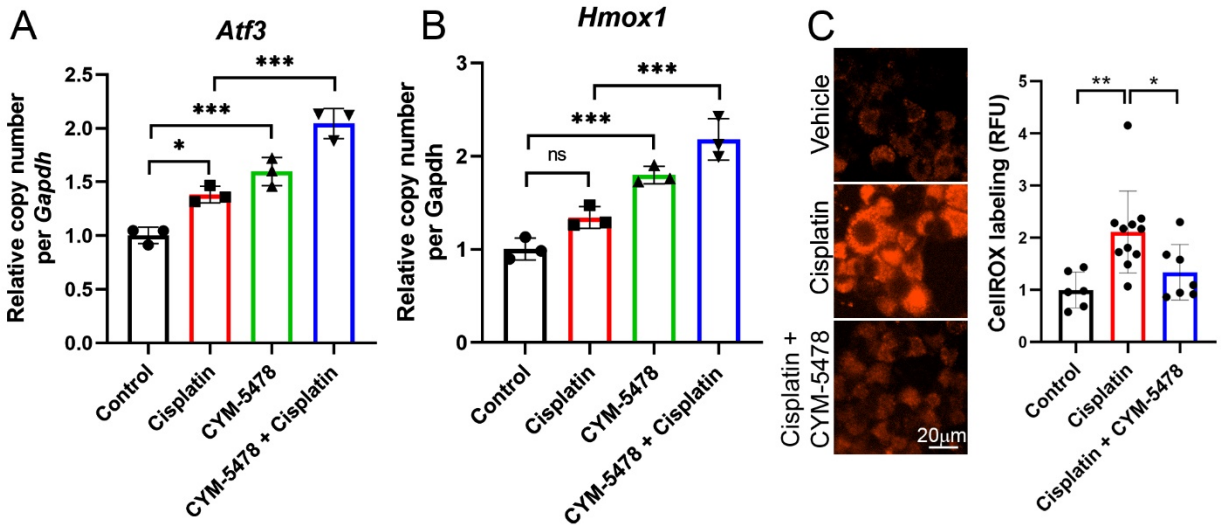

Figure 6: Expression of neuronal injury markers *in vitro*. Differentiated PC12 cells were treated overnight with 20 μM cisplatin, 10 μM CYM-5478, or both. Control cells were treated with vehicle only. Expression of *Atf3* (A) and *Hmox1* (B) were evaluated by qRT-PCR (N = 3). (C) ROS content was evaluated with the CellROX assay. Representative images are shown. Total fluorescence was quantified by ImageJ and depicted as relative fluorescence per cell (N = 6-11). ns = not significant, *P < 0.05, **P < 0.01, ***P < 0.001. Error bars represent standard deviations.

Activation of sphingosine 1-phosphate receptor 2 attenuates chemotherapy-induced neuropathy

Wei Wang, Ping Xiang, Wee Siong Chew, Federico Torta, Aishwarya Bandla, Violeta Lopez, Wei Lun Seow, Brenda Wan Shing Lam, Jing kai Chang, Peiyan Wong, Kanokporn Chayaburakul, Wei-Yi Ong, Markus R. Wenk, Raghav Sundar and Deron R Herr

J. Biol. Chem. published online December 27, 2019

Access the most updated version of this article at doi: 10.1074/jbc.RA119.011699